Available online at www.sciencedirect.com

SciVerse ScienceDirect

Energy Procedia 31 (2012) 167 – 172

Energy Procedia

E-MRS Spring Meeting 2011, Symposium S: Organic Photovoltaics: Science and Technology

Electroluminescence as characterization tool for polymer solar cells and modules

Marco Seeland[a], Roland Rösch[a], Burhan Muhsin[a], Gerhard Gobsch[a] and Harald Hoppe[a*]

[a]*Insitute of Physics, Ilmenau University of Technology, Weimarer Str. 32, 98673 Ilmenau, Germany*

Abstract

We show that laterally resolved luminescence detection is a highly versatile measurement technique for the characterization of polymer solar cells and modules. Besides lock-in thermography also luminescence imaging is highly suitable for quality control of processing steps, especially the control of homogeneous layer deposition and the proper lateral function of polymer solar cells and modules, by identification of local defects. Furthermore the application of luminescence imaging allows discrimination between active layer and organic/electrode-interface degradation in stability experiments. By correlation with photovoltaic parameters important conclusions can be drawn with respect to the specific degradation mechanism. For quantitative interpretation of such electroluminescence images, we propose an equivalent circuit model in which local solar cells are interconnected by resistors representing the sheet resistance of the transparent electrode. In combination with the laterally resolved measurement of electroluminescence, the application of this model allows calculation of local photovoltaic parameters and quantification of the lateral current and voltage distribution.

Keywords: imaging; organic photovoltaic; polymer; luminescence; degradation; characterization

1. Introduction

Laterally resolved luminescence detection with high-resolution cameras is a highly versatile method for solar cell characterization. Initially applied to silicon solar cells, luminescence imaging allows for

* Corresponding author. Tel.: +49 3677 69 3711; fax: +49 3677 69 3173.
E-mail address: harald.hoppe@tu-ilmenau.de.

doi:10.1016/j.egypro.2012.11.179

monitoring of the lateral distribution of minority-charge-carrier lifetime or diffusion length [1,2] and quasi-external series resistance [3]. Also for polymer based thin film solar cells the usability of luminescence imaging is highly versatile [4,5,6]. The currently best developed material system for polymer solar cells consists of a semiconducting polymer:fullerene composite such as poly-(3-hexylthiophene) (P3HT) and substituted methanofullerenes like [6,6]-phenyl-C_{61}-butyric acid methyl ester (PCBM) [7]. During the last few years also considerable higher power conversion efficiencies, recently exceeding 8%, have been achieved [8,9,10]. However, the lifetime of such devices plays a key role for the market entry as commercial products [11,12]. Since organic materials are very frail to chemical reactions with the ambient environment [13], especially with water and oxygen [14], the lifetime of unsealed devices is limited and therefore hermetical sealing and intrinsically more stable materials are required. We have shown recently that luminescence imaging, especially the combination of electroluminescence and photoluminescence imaging (ELI and PLI) yields valuable information about the local performance and allows investigating the degradation of the photovoltaic devices [4,15]. The non-invasive nature of this method allows time-resolved measurements of one and the same device stressed under continuous aging. Furthermore with ELI the injection and thus the electrode-organic interface, whereas with PLI the integrity of the organic semiconductor is tested, allowing the discrimination between active layer photooxidation and degradation of the cathode and the electrode/organic-interface [15]. For the continuative market entry along with improved quality control during the production of polymer solar modules, fast methods for the detection of defects are needed. Luminescence imaging has the potential for fast laterally resolved characterization within a few seconds. For the quantitative interpretation of electroluminescence images, we propose a Micro-Diode-Model (MDM) that is corresponding to the solar cell architecture and includes description of a semitransparent electrode with limited electrical conductivity. Operation in the series resistance limited regime leads to voltage losses over the length of the solar cell, causing inhomogeneous electroluminescence patterns. Furthermore the electroluminescence emission can be used for calculation of the local current and voltage distribution, which allows e.g. characterization of the sheet resistance of the semitransparent electrode.

2. Experimental

We applied luminescence imaging to P3HT:PCBM bulk heterojunction solar cells, with the active layer sandwiched between poly(3,4-ethylenedioxythiophene):poly(styrenesulfonate)/Indium Tin Oxide (PEDOT:PSS/ITO) and Aluminium electrodes (compare with Fig. 1a). Details of the device preparation are described elsewhere [7]. The method of luminescence imaging is based on the detection of luminescence radiation with a silicon charge-coupled-device (Si-CCD) camera as sketched in Fig. 1b. For electroluminescence imaging (ELI) a constant current at positive driving voltage was applied to the device under test. Thereby charge carriers were injected into the device resulting in a current flow of charges of both sign within the active layer, ultimately leading to radiative recombination with certain but small probability. For studying photoluminescence imaging (PLI) the devices were excited with a green solid-state diode emitting at 525 nm, leading to efficient photon absorption and exciton formation within the P3HT with subsequent radiative decay. To block the excitation light a cut-off filter was placed in front of the Si-CCD. Due to the efficient photoinduced charge transfer between P3HT and PCBM the photoluminescence was of low intensity as well. As the overall luminescence intensities are relatively small, the whole setup was placed into a light blocking housing.

For stability and degradation investigations, unsealed photovoltaic devices were aged in a controlled manner in a home-built stability setup that enables periodic in-situ IV-characterization. The stability setup consists of a high power illumination source (400W HQI-lamp), under which up to 40 solar cells can be placed. The solar cells were electrically connected to a computer-controlled source-measure-unit, and periodic *IV*-characterizations were sequentially performed on each solar cell by multiplexing.

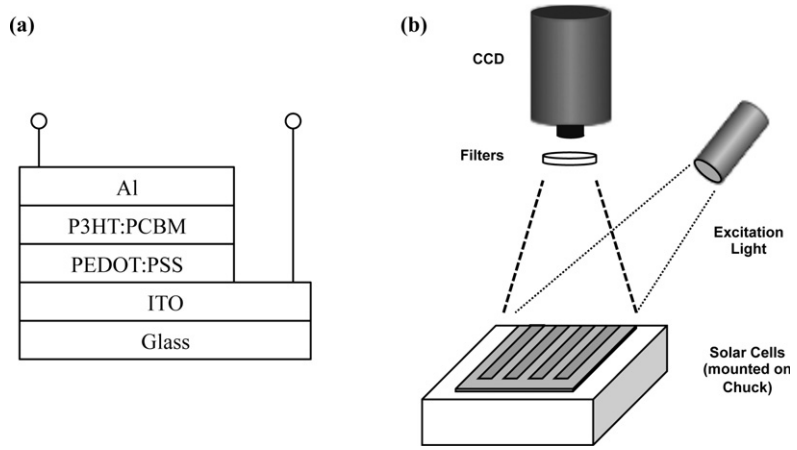

Fig. 1. (a) Schematic cross section of a P3HT:PCBM polymer solar cell. (b) Scheme showing the luminescence imaging setup. For ELI, charge carriers are injected into the device using a chuck with electrical contacts, whereas for PLI the device is illuminated by a light emitting diode through the glass/ITO-side, and optical filters are used to block the excitation light.

3. Results

3.1. Quality control by luminescence imaging

In previous publications, lock-in thermography was used for the quality control of polymer solar modules [16] and characterization of solar cells [17]. This technique allows detection of various processing deficiencies by laterally resolved detection of thermal radiation due to power dissipation, where especially shunts and active layer thickness variations can be precisely detected. It is shown here that also the detection of luminescence emitted from the organic semiconductor allows identification of especially active layer and cathode processing deficiencies. Therefore EL and PL images of a typical manually structured 2” x 2” polymer solar module [18] are shown in Fig. 2. Caused by the handling and spin coating process on a relatively large module area of 25 cm², various defects of different nature can be observed within both measurement modes. The highlighted defects in Fig. 2 include holes in the cathode as accidentally introduced by scratching (red ellipses) and handling induced defects (blue rectangles). Furthermore undissolved material and dust particles are observed (orange pentagons), which lead to defects during the film formation by spin coating and inhomogeneities in the active layer thickness. Due to the spin coating on the relatively large area, especially the corners of the module exhibit inhomogeneities in film thickness. Furthermore, a signal variation in the EL emission from the left to the right part of each cell in the module was observed, which will be discussed in section 3.3. It is interesting to note here that the module shown in Fig. 2 exhibits a relatively large fill factor of 59.9% and a power conversion efficiency of 2.1%, despite all defects. Minimizing the occurrence of processing problems therefore has great potential in further enhancing the efficiency.

3.2. Visualization of progressing degradation

Besides detection of processing deficiencies luminescence imaging is well suited for revealing defects occurring under aging of the photovoltaic devices [4]. The inhomogeneous degradation patterns of two unsealed solar cells kept for one week under ambient conditions either (a) under constant irradiation or (b) in the dark are shown in Fig. 3. Dark spots nucleated and grew with time in both cases, as detected by the ELI. The appearance of dark spots and the consecutive loss in electroluminescent area is attributed to

degradation of the cathode at the interface to the organic layer. The formation of aluminum oxide [19,20] followed by delamination of the cathode from the active layer [21,22] locally prohibits charge injection [23,24] and thus dark spots of circular shape are formed independently of any illumination.

On comparison of the photoluminescence images it is evident that especially in the case of illuminated storage the photoactive layer underwent photochemical degradation [25] at the sites locally corresponding to the electrode delamination (compare with Fig. 3a).

In conclusion, the combination of these two methods – ELI providing information on injection and thus the electrode-organic interface and PLI revealing the integrity of the organic semiconductor – allows discrimination between active layer photodegradation and corrosion of the electrodes.

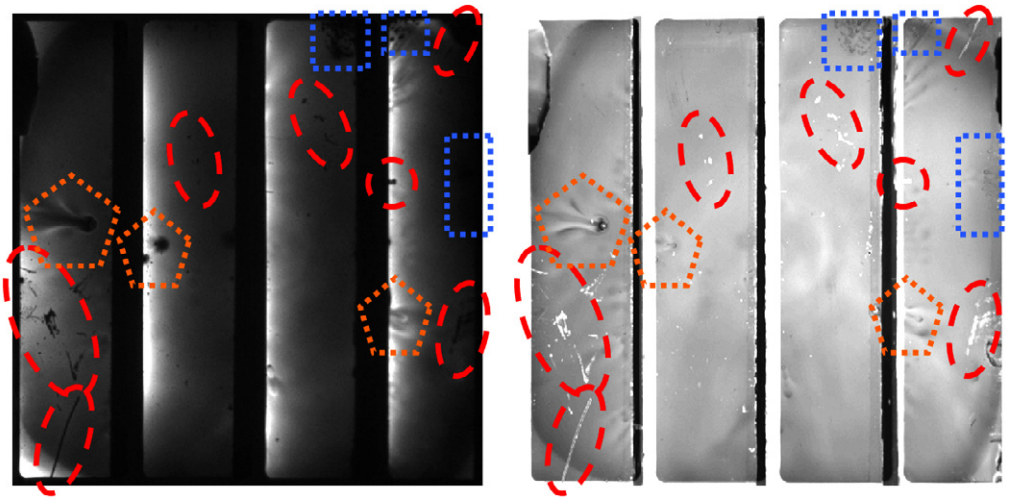

Fig. 2. EL (left) and PL (right) images of a 2" x 2" polymer solar module. Variuos defects, such as holes in the cathode (red ellipses) induced by scratches, handling problems (blue rectangles), undissolved materials and dust particles (orange pentagons) as well as film thickness inhomogeneities (note the increased signal in the corners) have been identified by the luminescence imaging.

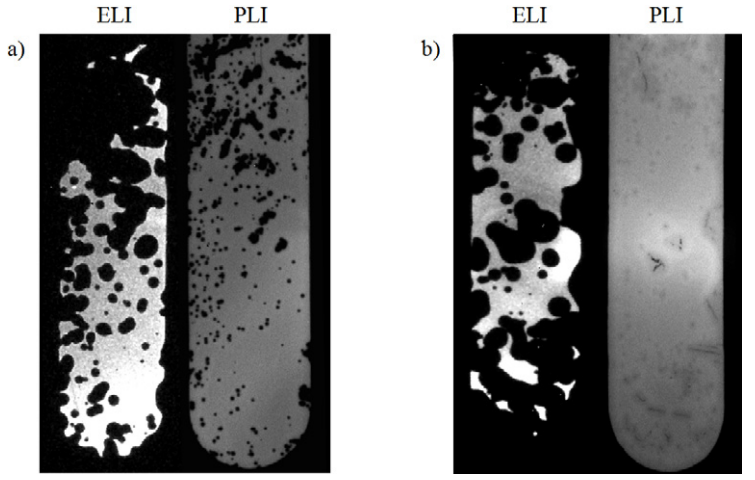

Fig. 3. EL and PL images for an unsealed device stored one week a) under 100 mW/cm² illumination and b) in the dark [4].

3.3. Quantitative Interpretation of EL images

Electroluminescence imaging reveals that the light emission clearly depends on the position with respect to the current transport direction along the length of the solar cell (compare with section 3.1.). This effect can be attributed to the limited conductivity of the semitransparent electrode, here Indium Tin Oxide (ITO), which is functioning as voltage divider and thereby reducing the electric potential acting on the photoactive layer [26,27]. As a result the local voltage is a function of the longitudinal position on the device with respect to the current transport direction along the solar cell length, yielding a highly inhomogeneous distribution of the injection current and consecutive EL emission [28].

To model the charge transport occurring in solar cells under forward bias, we propose the equivalent circuit model shown in Fig. 4. The model describes the active layer by diodes combined with series and parallel resistors. Neighboring nodes are connected by resistors representing the sheet-resistance of ITO [5]. For application of this Micro-Diode-Model (MDM) the electroluminescence intensity emitted from the solar cell is used for calculating the local current flow through each node. The resulting current distribution through each circuit element can be readily fitted using the Kirchhoff's laws for the junction voltages V_N and the node currents I_N. Details of the calculations and computational steps are given in Ref. [5].

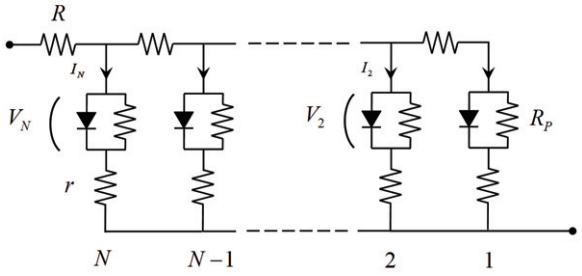

Fig. 4. Micro-Diode-Model used for quantitative description of the measured EL distribution. The active layer is modeled by diodes with series and parallel resistors. Neighboring nodes are interconnected by resistors representing the sheet-resistance of ITO.

The proposed MDM allows precise description of the current and voltage distribution [5]. In Fig. 5, experimental and calculated current profiles along the length of a solar cell are shown together with the calculated voltage profile. From these calculations, e.g. the sheet-resistance of the ITO electrode can be extracted, which was found to be in very good agreement with experimentally determined sheet-resistance values [29,30].

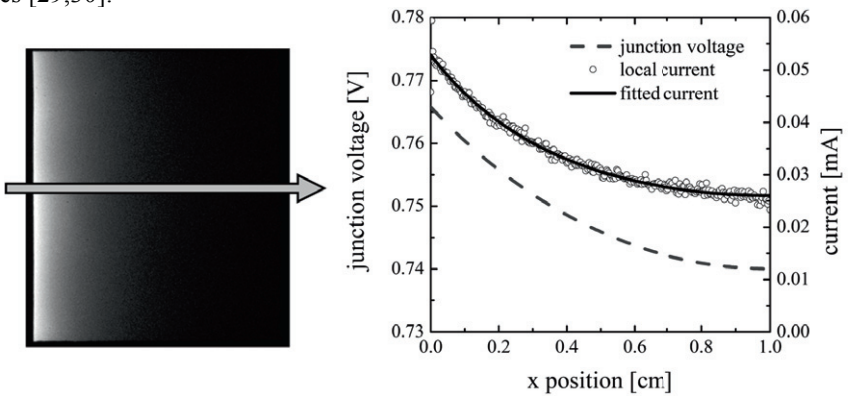

Fig. 5. Fitting the MDM to the local current profile along the length of the solar cell as calculated from the EL intensity (image on the left and empty dots in plot on the right) allows calculation of the local current and junction voltage profiles.

4. Conclusions

The application of luminescence imaging yields valuable information for the spatially resolved characterization of polymer solar cells and modules. It is highly suitable for the identification of local defects in the photoactive layer or on the electrodes e.g. caused by processing deficiencies. Local degradation can be detected allowing the discrimination between electrode-interface and active layer failure processes. Beyond that, the lateral EL emission can be used for a quantitative description of the local junction voltage and current flow, where the geometry of the device and the sheet-resistance of the semitransparent electrode are the key factors for inhomogeneous light emission.

Acknowledgements

The authors are grateful for financial support from the Thuringian Ministry of Culture and the German Federal Ministry of Education and Research in the frameworks of FIPV II and PPP (contract number 13N9843), respectively.

References

[1] P. Würfel, T. Trupke, T. Puzzer, E. Schäffer, W. Warta, and S. W. Glunz, J. Appl. Phys. **101**, 123110 (2007).
[2] J.A. Giesecke, M. Kasemann and W. Warta, J. Appl. Phys. **106**, 014907 (2009).
[3] T. Trupke, E. Pink, R.A. Bardos and M.D. Abbott, Appl. Phys. Lett. **90**, 093506 (2007).
[4] M. Seeland, R. Rösch, H. Hoppe, J. Appl. Phys. **109**, 064513 (2011).
[5] M. Seeland, R. Rösch, H. Hoppe, submitted.
[6] U. Hoyer, M. Wagner, Th. Swonke, J. Bachmann, R. Auer, A. Osvet, C.J. Brabec, Appl. Phys. Lett. 97, 233303 (2010).
[7] J.A. Renz, T. Keller, M. Schneider, S. Shokhovets, K.D. Jandt, G. Gobsch et al., Sol. Energy Mater. Sol. Cells **93**, 508 (2009).
[8] http://www.forbes.com/feeds/businesswire/2010/07/27/businesswire142993163.html
[9] Y. Liang, Z. Xu, J. Xia, S.-T. Tsai, Y. Wu, G. Li, et al., Adv. Mater. **22**, E135 (2010).
[10] R.F. Service, Science **332**, 293 (2011).
[11] C.J. Brabec, Sol. Energy Mater. Sol. Cells **83**, 273 (2004).
[12] T.D. Nielsen, C. Cruickshank, S. Foged, J. Thorsen and F.C. Krebs, Sol. Energy Mater. Sol. Cells **94**, 1553 (2010).
[13] F.C. Krebs and K. Norrman, Prog. Photovolt: Res. Appl. **15**, 697 (2007).
[14] K. Kawano, R. Pacios, D. Poplavskyy, J. Nelson, D.D.C. Bradley and J.R. Durrant, Sol. Energy Mater. Sol. Cells **90**, 3520 (2006).
[15] I.G. Scheblykin, V.I. Arkhipov, M. Van der Auweraer, F. De Schryver, HELV CHIM ACTA **84**, 3616 (2001).
[16] H. Hoppe, J. Bachmann, B. Muhsin, K.-H. Drüe, I. Riedel, G. Gobsch et al., J. Appl. Phys. **107**, 014505 (2010).
[17] J. Bachmann, C. Buerhop-Lutz, C. Deibel, I. Riedel, H. Hoppe, C.J. Brabec et al., Sol. Energy Mater. Sol. Cells **94**, 642 (2010).
[18] B. Muhsin, J. Renz, K.-H. Drüe, G. Gobsch, H. Hoppe, Synthetic Met. **159**, 2358 (2009).
[19] S.F. Lim, L. Ke, W. Wang and S.J. Chua, Appl. Phys. Lett. **78**, 2116 (2001).
[20] M. Schaer, F. Nuesch, D. Berner, W. Leo and L. Zuppiroli, Adv. Func. Mater. **11**, 116 (2001).
[21] C.W.T. Bulle-Lieuwma, P. van de Weijer, Appl. Surf. Sci. **252**, 6597 (2006).
[22] M. Fujihira, L.M. Do, A. Koike, and E.M. Han, Appl. Phys. Lett. **68**, 1787 (1996).
[23] D. Kolosov, D.S. English, V. Bulovic, P.F. Barbara, S.R. Forrest and M.E. Thompson, J. Appl. Phys. **90**, 3242 (2001).
[24] S.Y. Kim, K.Y. Kim, Y.J. Tak and J.L. Lee, Appl. Phys. Lett. **89**, 132108 (2006).
[25] K. Norrman, N.B. Larsen and F.C. Krebs, Sol. Energy Mater. Sol. Cells **90**, 2793 (2006).
[26] A. de Vos, Sol. Cells **12**, 311 (1984).
[27] G.T. Koishiyev and J.R. Sites, Sol. Energy Mater. Sol. Cells **93**, 350 (2009).
[28] K. Neyts, M. Marescaux, A.U. Nieto, A. Elschner, W. Lövenich, K. Fehse et al, J. Appl. Phys. **100**, 114513 (2006).
[29] B. Muhsin, J. Renz, K.-H. Drüe, G. Gobsch, H. Hoppe, Phys. Status Solidi A **12**, 2771 (2009).
[30] H. Hoppe, M. Seeland, B. Muhsin, G. Gobsch, in preparation.